



## HHS PUBLIC ACCESS

Author manuscript

*Bioorg Med Chem.* Author manuscript; available in PMC 2017 November 15.

Published in final edited form as:

*Bioorg Med Chem.* 2016 November 15; 24(22): 6048–6057. doi:10.1016/j.bmc.2016.09.062.

## Triethylated chromones with substituted naphthalenes as tubulin inhibitors

Kyoko Nakagawa-Goto<sup>a,b,\*</sup>, Yukako Taniguchi<sup>a</sup>, Yurie Watanabe<sup>a</sup>, Akifumi Oda<sup>a</sup>, Emika Ohkoshi<sup>b</sup>, Ernest Hamel<sup>c</sup>, Kuo-Hsiung Lee<sup>b,d</sup>, and Masuo Goto<sup>b,\*</sup>

<sup>a</sup>School of Pharmaceutical Sciences, College of Medical, Pharmaceutical and Health Sciences, Kanazawa University, Kanazawa, 920-1192, Japan

<sup>b</sup>Natural Products Research Laboratories, UNC Eshelman School of Pharmacy, University of North Carolina, Chapel Hill, North Carolina 27599-7568, United States

<sup>c</sup>Screening Technologies Branch, Developmental Therapeutics Program, Division of Cancer Treatment and Diagnosis, Frederick National Laboratory for Cancer Research, National Cancer Institute, Frederick, Maryland, 21702, United States

<sup>d</sup>Chinese Medicine Research and Development Center, China Medical University and Hospital, 2 Yuh-Der Road, Taichung, 40447, Taiwan

### Abstract

Previously synthesized 2-(benzo[*b*]thiophene-3'-yl)-6,8,8-triethyl-desmosdumotin B (**1**, TEDB-TB) and 2-(naphth-1'-yl)-6,8,8-triethyl-desmosdumotin B (**2**) showed potent activity against multiple human tumor cell lines, including a multidrug-resistant (MDR) subline, by targeting spindle formation and/or the microtubule network. Consequently, ester analogues of hydroxylated naphthyl substituted TEDBs (**3–5**) were prepared and evaluated for their effects on tumor cell proliferation and on tubulin assembly. Among all new compounds, compound **6**, a 4'-acetoxynaphthalen-1'-yl derivative, displayed the most potent antiproliferative activity (IC<sub>50</sub> 0.2–5.7 μM). Selected analogues were confirmed to be tubulin assembly inhibitors in cell-free and cell-based assays using MDR tumor cells. The new analogues partially inhibited colchicine binding to tubulin, suggesting their binding mode would be different from that of colchicine. This observation was supported by computational docking model analyses. Thus, the newly synthesized triethylated chromones with esterified naphthalene groups have good potential for development as a new class of mitotic inhibitors that target tubulin.

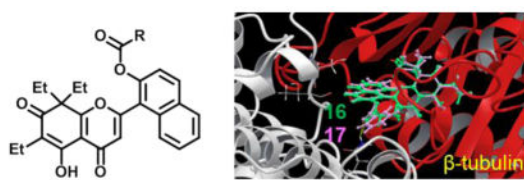
### Graphical abstract

\*Corresponding authors. K.N.G. Tel.: 81-76-264-6305, kngoto@p.kanazawa-u.ac.jp, MG. Tel.: 919-843-6325, goto@med.unc.edu.

Supplementary data

Supplementary data [NMR and MS spectra of compounds **6–22** (PDF)] associated with this article can be found, in the online version,

**Publisher's Disclaimer:** This is a PDF file of an unedited manuscript that has been accepted for publication. As a service to our customers we are providing this early version of the manuscript. The manuscript will undergo copyediting, typesetting, and review of the resulting proof before it is published in its final citable form. Please note that during the production process errors may be discovered which could affect the content, and all legal disclaimers that apply to the journal pertain.



R (Comp.)	Distance to aa on $\beta$ -tubulin (Å)				IC <sub>50</sub> tubulin assembly
	Asn249	Lys254	Thr314	Asn350	
Et ( <b>16</b> )	>5	>5	>5	>5	2.3 $\mu$ M
Ph ( <b>17</b> )	3.8	3.8	4.9	5.3	>20.0 $\mu$ M
CH=CHPh ( <b>18</b> )	3.8	3.3	3.1	3.2	>20.0 $\mu$ M

## 1. Introduction

The structural diversity of natural products (NPs) has contributed significantly to past drug discovery. In their recent review, Newman and Cragg stated that NPs are still playing a dominant role in the current discovery of leads and development of drugs for the treatment of human diseases.<sup>1</sup> The biosynthesis of NPs occurs efficiently via well-controlled reactions promoted by natural enzymes, while chemical syntheses of NPs are not always easy. Nonetheless, novel bioactive compounds that are biosynthetically not observed can be artificially produced as synthetic NP derivatives. Thus, the application of organic synthesis to core NP skeletons can supply richer structural variety to expand the possibility of potent drug leads. The chemical modification of lead natural products is also a useful strategy to improve the desired pharmacological activity and to reduce adverse clinical side effects. The differences in functional groups and their positions can affect various drug parameters, such as partition coefficient, electron density, structure conformation, bioavailability, and other pharmacokinetics factors involved in the interaction between ligand and cellular targets. We selected novel scaffolds that do not occur biosynthetically but can be converted to promising drug candidates, based on chemical modification of natural skeletons.

Aromatic ring systems are key scaffolds in medicinal chemistry, because their electron rich  $\pi$  systems and structurally rigid planar frameworks can often play a critical role in the interactions of ligands with their cellular targets. A phenyl group is the most common aromatic ring found in natural products. However, bicyclic aromatic systems, such as naphthalene, have expanded  $\pi$  orbitals, which can sometimes lead to dramatic changes in ligand–receptor interactions. It was reported previously that the biological profile of triethyl-desmosdumotin B (TEDB) could be significantly changed based on the identity of the B-ring (Figure 1).<sup>2,3</sup> When the pendant B-ring was a  $6\pi$ -electron aromatic system, the TEDB analogue showed effective cytotoxicity only against p-glycoprotein (P-gp) overexpressing multi-drug resistant (MDR) cells, but no cytotoxicity against any chemosensitive tumor cell line.<sup>2–5</sup> In contrast, compounds with a  $10\pi$ -rather than  $6\pi$ -electron aromatic system, such as 2-(benzo[*b*]thiophene-3'-yl)-6,8,8-triethyl-desmosdumotin B (**1**, TEDB-TB) and 2-(naphth-1'-yl)-6,8,8-triethyl-desmosdumotin B (**2**), exhibited potent antiproliferative activity against multiple human cancer cell lines, including MDR tumor cells, acting via inhibition of tubulin polymerization, in part through the colchicine site

(CS).<sup>6</sup> It was also found that hydroxylated benzothiophene analogues efficiently induced cell cycle arrest at the G2/M phase, with formation of immature multipolar spindles.<sup>7</sup>

To explore the biological potential of this compound class, we have continued the investigation of TEDB derivatives. A hydroxy group provides a polar surface on the naphthalene molecule, which has no topological polar surface area (TPSA) by itself. Hydroxy naphthalene derivatives **3–5**, which were already in hand,<sup>7</sup> could be easily esterified to produce various ester derivatives. Acyl group might contribute to H-bond interactions with the target protein or could provide a spacer element. Furthermore, the functional group differences might alter the biological profile, as we previously described.<sup>2–7</sup>

An ester group plays an important role in biological activity. A well-known instance is paclitaxel (PXL), an antitumor drug in clinical use. The ester side chain at position C-13, acetate at position C-4, and benzoate at position C-2 are essential for the antitubulin activity of PXL.<sup>8</sup> Analogues without ester groups at the above mentioned positions or with simplified side chains at C-13 have dramatically reduced activity.

The antiproliferative activities of all new TEDB derivatives against several cancer cell lines, including an MDR cell line, were studied. Selected analogues were investigated for potential inhibitory effects on tubulin assembly with purified tubulin and for effects on cell cycle progression in human tumor cells.

## 2. Results and discussion

### 2.1. Chemistry

The hydroxylated analogues **3–5** were synthesized previously (Scheme 1).<sup>7</sup> Esterifications of **3–5** were accomplished using the appropriate acyl chloride for **6–22**. The structures and purities of all synthesized compounds were confirmed by <sup>1</sup>H-NMR, high resolution MS, and HPLC analysis.

### 2.2. Biological evaluation and structure–activity relationship

**2.2.1. Antiproliferative activity**—Newly synthesized analogues **3–22** were tested for antiproliferative activity against eight human tumor cell lines, A549 (lung carcinoma), HCT-8 (colon adenocarcinoma), Hep G2 (hepatocellular carcinoma), PC-3 (prostate cancer), DU 145 (prostate cancer), SK-BR-3 (HER2-overexpressing breast cancer), KB (originally isolated from epidermoid carcinoma of the nasopharynx), and KB-subline KB-VIN showing MDR phenotype with overexpression of P-gp (Table 1). The antiproliferative effects of compounds were determined by the sulforhodamine B (SRB) assay, and IC<sub>50</sub> values were calculated from at least three independent experiments with duplication. The antiproliferative activities of the compounds **2–5** are also shown for comparison. A cytotoxic P-gp substrate, PXL, was used as an experimental control. The selected analogues were also tested with purified tubulin for inhibitory effects on its assembly and on the binding of [<sup>3</sup>H]colchicine. The 50% effective concentration for inhibiting tubulin assembly (EC<sub>50</sub>-ITA) and percent inhibition of colchicine binding to tubulin (ICB) in the presence of tested compounds are also presented in Table 1. Combretastatin A-4 (CA-4), a colchicine-type

antitubulin agent, was used as a positive control for ITA ( $EC_{50} = 1.1 \mu\text{M}$ ) and ICB (99% inhibition).

From the results with analogues **3** and **4**, hydroxylation at the 4'-position (**3**) of 2'-naphthyl-TEDB **2** effectively enhanced the cell growth inhibition in A549, Hep G2, KB and KB-VIN cell lines ( $IC_{50}$  0.9, 0.4, 0.7, and 0.5  $\mu\text{M}$ , respectively), while hydroxylation at the 2'-position (**4**) had less effect ( $IC_{50}$  1.2, 1.6, 1.0, and 1.0  $\mu\text{M}$ , respectively). The latter potencies were closer to those of the parent **2**.<sup>7</sup> Although the antiproliferative activities of **3** and **4** were slightly different, their ITA and ICB potencies using a cell free system were comparable. In contrast, the 6'-hydroxy-1'-naphthyl-TEDB analogue (**5**) exhibited marginal antiproliferative potency.

Except **22**, all tested compounds exhibited some antiproliferative activity ( $IC_{50}$  less than 20  $\mu\text{M}$ ) against KB-VIN, a P-gp-overexpressing MDR tumor cell line. Therefore, these analogues are not P-gp substrates and can be effective against MDR tumors. Notably, the antiproliferative activity of cinnamoyl ester **13** against KB-VIN was eightfold greater than that against KB, the parent non-MDR tumor cell line.

Esterifications of naphthols **3** and **4** successfully increased or preserved the antiproliferative effects in most cases. Especially, acetate **6** exhibited significantly improved antiproliferative activity against all tested cell lines, except DU 145 and SK-BR-3. The observed  $IC_{50}$  values of 0.2 to 0.5  $\mu\text{M}$  were better than those of the parent **3**. Benzoate **12** and acetate **6** inhibited tumor cell growth with similar potency, but **12** was slightly less active than **6** against KB-VIN. Interestingly, benzoate **12** and propionate **7** did not inhibit tubulin assembly as opposed to **3** and acetate **6**, although all four compounds showed potent antiproliferative activity. Unlike other esters of naphthol **3**, compounds **9–11** displayed impressive activity against DU 145 and SK-BR-3. Among the ester analogues of **4**, acetate **15** demonstrated slightly better activity than the parent alcohol **4**. Other analogues showed similar antiproliferative activity, but benzoate **17** and cinnamate **18** did not inhibit tubulin assembly. All four ester analogues (**19–22**) of 6'-naphthol **5** showed no significant improvement in antiproliferative activity as compared with the parent compound.

Selected active compounds were tested for potential inhibition of tubulin assembly. Analogues **3**, **4**, **6**, and **16** inhibited tubulin assembly and modestly inhibited colchicine binding, while CA-4 caused 98% inhibition (data not shown) at the inhibitor concentration used. This observation suggested that these compounds might target tubulin in a different manner from CS-binding agents.

**2.2.2. Effects on cell cycle**—Because induction of cell cycle arrest at G2/M is one of the typical effects of tubulin inhibitors on tumor cells, the effect of the newly synthesized compounds on cell cycle progression by using flow cytometry was investigated (Figure 2). Antimitotic natural products such as colchicine, VIN and PXL inhibit cell cycle progression at the G2/M phase in chemosensitive tumors. However, these three compounds are ineffective against MDR tumors overexpressing ABC transporter(s).<sup>7</sup> The newly synthesized compounds suppressed MDR and chemosensitive cell growth at the same concentrations, we analyzed the cell cycle progression of KB-VIN cells treated with selected analogues,

including **7**, **12** and **18**, which showed little or no effects on the assembly of purified tubulin. As shown in Figure 2, except **13**, all tested compounds induced cell cycle arrest at the G2/M phase within 24 h. Analogues **7**, **12** and **18**, which had tubulin assembly EC<sub>50</sub> values > 20.0 μM, also induced cell cycle arrest at G2/M, suggesting that these compounds may be activated in the cells or have a target other than tubulin. These results also suggest that the more selective antiproliferative effect of **13** against KB-VIN as compared with KB may not have been caused by an impact on the cell cycle, but may target a protein other than tubulin, such as a MDR-related protein responsible for cell growth. Further mechanism of action studies are required to elucidate a unique bioactivity of **13**.

To study further the effects of the analogues on microtubules and spindle formations, as well as to determine their point of impact on the cell cycle, treated KB-VIN cells were labeled with antibodies against α-tubulin and serine 10-phosphorylated histone H3 (p-H3) as a mitotic chromosome condensation marker and with 4',6-diamidino-2-phenylindole (DAPI), which labels DNA (Figure 3). In the DMSO-treated control cells, p-H3-positive mitotic cells displayed normal bipolar spindle formation, and normal microtubule networks without p-H3 labeling were present in interphase. In contrast, in cells treated with compounds **3**, **4**, **16** or **18**, abnormal multipolar spindles were often present in the chromosome-condensed p-H3-positive mitotic cells, while disrupted microtubules were observed in interphase cells. Dose increases stimulated these microtubule defects, suggesting a dose-dependent manner of action. Multiple α-tubulin accumulated spots in p-H3-positive cells were obvious following treatment with **4** or **18**, demonstrating that these analogues disrupt spindle formation and amplify the spindle poles at prometaphase. These observations support the flow cytometry results that showed induction of cell cycle arrest at G2/M. Based on these immunostaining studies, bipolar spindle formation was almost eliminated, confirming that the cells were arrested at prometaphase. Multipolar spindle formations were obvious in the mitotic cells, while undetectable in CA-4-treated cells. These phenotypes were clearly different from that of CA-4-treated cells, suggesting that our analogues exert a different mechanism of action than does CA-4.

Furthermore, analogue **18**, which had an EC<sub>50</sub> > 20.0 μM for inhibition of purified tubulin assembly, also showed the same phenotype as analogues **4** and **16**. These results suggest that **18** may be biologically activated in the cell-based assay to target tubulin to cause the arrest of cells at prometaphase with induction of multipolar spindles.

**2.2.3 Induction of nuclear fragmentation**—In the course of phenotypic analysis, we found that compounds **4** and **18** induced nuclear fragmentation (Figure 4, yellow arrows), while such fragmentation was undetectable in cells treated with **16** (Figure 3). Fragmented nuclei from treatment with **4** were negative against an antibody to p-H3, suggesting that the fragmentation was induced at interphase. In contrast, fragmented nuclei from **18** were stained with an antibody to p-H3 (blue arrows), suggesting that fragmentation was induced after the onset of chromosome condensation. As mentioned above, we believe that **18** is most likely biologically activated in the cells. This activation process could produce multiple forms of **18**-related bioactive compounds, and one of these could show similar effects to those observed with **4**. Unfortunately, it is still unclear whether the nuclear fragmentation

was a consequence of tubulin inhibitory effects, because nuclear fragmentation was not detected in cells treated with **16** or CA-4. Further mechanism of action studies are required to address this point and compounds **4** and **18** may have more than one target.

**2.2.4. Docking models of compounds**—The immunocytochemical evaluations described above demonstrated that the new analogues affected microtubule polymerization and especially induced dysfunction of bipolar spindle formation. These phenotypes are similar to but significantly different from those observed with CA-4. In fact, interphase microtubules as well as spindles and their poles were totally depolymerized by CA-4, while amplified spindle poles and immature multiple spindles were formed by treatment with synthetic analogues (Figure 3). Based on these observations, we predicted that our new analogues targeted the CS on tubulin, but in a different docking mode from that of colchicine. Previously, we reported a theoretical binding mode of TEDB-TB analogues docked into the CS through hydrogen bonds (H-bonds) formed with both  $\alpha$ - and  $\beta$ -tubulins without interfering with colchicine binding.<sup>7</sup> Thus, we employed computer modeling using the tubulin crystal structure (PDB ID: 1SAO) in the current study.

4'-Naphthol **3** and its acetate **6**, which inhibited the assembly of purified tubulin, were computationally docked within the CS (Figure 5A). As we expected, the detailed docking model revealed that three oxygen atoms on the chromone skeletons of **3** and **6** formed H-bonds with Asn101, Ser178, and Thr179 on  $\alpha$ -tubulin (Figure 5B). Propionyl ester **7**, which has only one additional carbon atom as compared with acetate **6**, but had an  $EC_{50} > 20.0 \mu\text{M}$  in the purified tubulin assembly assay, could be similarly docked into the CS. However, it was conceivable that the propionyl side chain on the naphthalene ring had unfavorable steric interactions with Leu252 and Leu255 on  $\beta$ -tubulin, resulting in **7** being incapable of docking within the CS (dotted circle in Figure 5C). Distances of 5.33 and 4.44 Å were calculated between the terminal methyl group of the acetyl side chain of **6** with  $\beta$ Leu252 and  $\beta$ Leu255, respectively. In comparison, the terminal methyl group of the propionyl moiety of **7** was closer to  $\beta$ Leu252 and  $\beta$ Leu255, with calculated distances of 3.84 and 3.80 Å, respectively (Figure 5D). These observations could support the differing results in the tubulin assembly assay, in which **6** and **7** had  $EC_{50}$ 's of 2.4 and  $> 20 \mu\text{M}$ , respectively (Table 1, ITA).

The docking studies on the 2'-ester analogues with the CS was also consistent with the distinctive bioactivities of the different analogues in the tubulin assembly assay. In the overlapped docking modes of **4** and CA-4, **4** formed three H-bonds with  $\alpha$ Asn101,  $\alpha$ Ser178 and  $\alpha$ Thr179, while CA-4 formed only one H-bond with  $\alpha$ Ser178 (Figures 6A, B). This difference could result in the apparently different impacts on tubulin assembly, as well as the different phenotypes observed in compound-treated cells at the onset of mitosis. The superimposition of docked **16** demonstrated that only one H-bond would be formed between the ester carbonyl group and  $\alpha$ Asn101 (Figure 6C). No H-bonds were possible with  $\alpha$ Ser178 and  $\alpha$ Thr179, because the naphthyl ring directly faced these residues. In the predicted docking models of **16** and **17** in the CS, the benzoate phenyl ring of **17** was quite close to  $\beta$ Asn249 and  $\beta$ Lys254, likely resulting in steric obstruction, while the propionyl side chain of **16** seemed to have adequate space near these two residues (Figure 6D). These results indicated that the docking of **17** into the CS would be improbable as compared with



**16**, supporting the results from the tubulin assembly assay, in which **16** had an  $EC_{50}$  of 2.3  $\mu\text{M}$ , while **17** had an  $EC_{50} > 20.0 \mu\text{M}$ . In addition, superimposition of **18** into the CS showed no H-bond formation, suggesting that **18** would be incapable of docking into the CS (Figure 6E). These differences in the modeling study reflect the differences in the tubulin assembly assay, where 2'-naphthol **4** and propionate **16** inhibited tubulin assembly, while benzoate **17** and cinnamate **18** yielded  $EC_{50}$  values  $> 20.0 \mu\text{M}$ .

The best-scored docking models of compounds **4**, **16**, **17**, and **18** within the CS were analyzed for potential predictive utility with the tubulin assembly assay. These four compounds were selected because **4** and **16** were good inhibitors, while **17** and **18** had little if any inhibitory activity (see ITA values in Figure 7A). The binding ability of each ligand in the CS was evaluated by H-bond formation (Figures 5A–C and 6A–C). Furthermore, steric hindrance between the ligand and the tubulin amino acid residues was also considered as a critical binding factor (Figures 5D, 6D). The distances between the compound and the amino acid residues, especially  $\beta\text{Asn}249$ ,  $\beta\text{Lys}254$ ,  $\beta\text{Thr}314$ , and  $\beta\text{Asn}350$ , on  $\beta$ -tubulin in the CS are summarized in Figure 7B. No significant steric hindrance was anticipated for **4** and **16**, with over 5 Å distances from the amino acid residues. However, while the phenyl group on the benzoate of **17** has adequate distances from  $\beta\text{Thr}314$  (4.94 Å) as well as  $\beta\text{Asn}350$  (5.32 Å), the phenyl group on the cinnamate of **18** is quite close to  $\beta\text{Thr}314$  (3.11 Å) and  $\beta\text{Asn}350$  (3.15 Å). Both the benzoate group of **17** as well as the naphthyl of **18** are close to  $\beta\text{Asn}249$  (3.81 and 3.76 Å, respectively) and  $\beta\text{Lys}254$  (3.83 and 3.34 Å, respectively), which may obstruct docking. These analyses suggest that the additional phenyl group on the naphthalene might not bind to the CS due to the steric hindrance. This reasoning also concurs with the finding that **17** and **18** yielded  $EC_{50}$ 's  $> 20.0 \mu\text{M}$  in the tubulin assembly assay. Thus, our docking models could be useful in the design of a new CS agent by calculating potential for H-bond formation and steric hindrance.

### 3. Conclusions

In summary, new ester analogues **5–22** from hydroxy TEDB-TBs **3–5** were synthesized, and their biological activities were evaluated. All ester analogues derived from **3** and **4**, except **8**, showed significant antiproliferative activity against multiple tumor cell lines, including the MDR line. Acetate, propionate, and benzoate analogues exhibited more potent activity than the parent compounds, **3** and **4**. These cytotoxic analogues induced cell cycle arrest at the G2/M phase, and the arrest was at prometaphase by disrupting bipolar spindle formation. Amplification of spindle poles resulted in the formation of multipolar spindles observed in cells treated with the most potent compounds. This phenotype is different from that of other CS agents, such as CA-4, and characteristic of TEDB analogues. Computer-assisted docking modes of compound binding to the CS suggested that modified TEDB analogues and colchicine bind to the CS via different binding modes. We found that predicted H-bond formation and steric hindrance between compound and amino acid residues in the CS was consistent with the observed inhibitory effects on tubulin assembly. The contradictions between cell-free and cell-based antitubulin effects, such as found with compounds **7**, **12**, and **18**, can possibly be explained by the biological activation of these analogues in the cancer cells. These analogues may have potential for the development of anticancer

prodrugs. Thus, our docking models combined with bioactivity results may be useful for the design of a novel prodrug targeting tubulin.

## 4. Experimental sections

### 4.1. Chemistry

**4.1.1. General Experimental Procedures**—All chemicals and solvents were used as purchased. All melting points were measured on a Fisher-Johns melting point apparatus without correction.  $^1\text{H}$  and  $^{13}\text{C}$  NMR spectra were recorded on a Varian Gemini 2000 (300 MHz) or a Varian Inova (400 MHz, 600 MHz) NMR spectrometer with TMS as the internal standard. All chemical shifts are reported in ppm. NMR spectra were referenced to the residual solvent peak, chemical shifts  $\delta$  in ppm, apparent scalar coupling constants  $J$  in Hz. Mass spectroscopic data were obtained on a Shimadzu LCMS-IT-TOF instrument or JMS-700 MStation (FAB). Analytical thin-layer chromatography (TLC) was carried out on Merck precoated aluminum silica gel sheets (Kieselgel 60 F-254). Teledyne Isco Combiflash system was used for flash chromatography. All target compounds were characterized and determined as at least >95% pure by  $^1\text{H}$ -NMR, HRMS, and analytical HPLC.

**4.1.2. General Synthetic Procedures for Esterification**—To a solution of hydroxy TEDB analogues (**3–5**) in  $\text{CH}_2\text{Cl}_2$ ,  $\text{Et}_3\text{N}$  (2.0 equiv. mol) and the related acyl chloride (1.1 equiv. mol) were added at 0 °C. The mixture was stirred at 0 °C for 1.5 h. The reaction mixture was quenched with saturated aq.  $\text{NH}_4\text{Cl}$  and extracted with  $\text{CH}_2\text{Cl}_2$ . The extract was washed with brine, dried over  $\text{Na}_2\text{SO}_4$ , and concentrated *in vacuo*. The residue was purified by silica gel chromatography with EtOAc–hexane as eluent to afford the related esters **6–22**.

**4.1.2.1. 4'-Acetoxynaphthalen-1'-yl-TEDB (6):**  $^1\text{H}$  NMR (400 MHz,  $\text{CDCl}_3$ )  $\delta$  13.00 (1H, s, chelated-OH), 8.08–8.01 (1H, m, naphthalene-H), 7.98–7.91 (1H, m, naphthalene-H), 7.69 (1H, d,  $J = 7.7$  Hz, 2'-H), 7.73–7.69 (2H, m, naphthalene-H), 7.40 (1H, d,  $J = 7.7$  Hz, 3'-H), 6.80 (1H, s, 3-H), 2.53 (3H, s), 2.53–2.43 (2H, m), 2.24–2.14 (2H, m), 1.96–1.84 (2H, m), 1.06 (3H, t,  $J = 7.3$  Hz), 0.73 (6H, t,  $J = 7.3$  Hz). HRMS  $m/z$  447.1791 [ $\text{M}+\text{H}$ ] $^+$  (calcd for  $\text{C}_{27}\text{H}_{26}\text{O}_6$ , 447.1802).

**4.1.2.2. 4'-Propionyloxynaphthalen-1'-yl-TEDB (7):**  $^1\text{H}$  NMR (600 MHz,  $\text{CDCl}_3$ )  $\delta$  13.02 (1H, s, chelated-OH), 8.06–8.03 (1H, m, naphthalene-H), 7.96–7.93 (1H, m, naphthalene-H), 7.69 (1H, d,  $J = 8.0$  Hz, 2'-H), 7.67–7.61 (2H, m, naphthalene-H), 7.41 (1H, d,  $J = 8.0$  Hz, 3'-H), 6.81 (1H, s, 3-H), 2.84 (2H, q,  $J = 7.4$  Hz), 2.49 (2H, q,  $J = 7.4$  Hz), 2.23–2.16 (2H, m), 1.93–1.86 (2H, m), 1.41 (3H, t,  $J = 7.4$  Hz), 1.06 (3H, t,  $J = 7.4$  Hz), 0.72 (6H, t,  $J = 7.4$  Hz). HRMS  $m/z$  461.1964 [ $\text{M}+\text{H}$ ] $^+$  (calcd for  $\text{C}_{28}\text{H}_{28}\text{O}_6$ , 461.1959).

**4.1.2.3. 4'-Isovaleryloxynaphthalen-1'-yl-TEDB (8):**  $^1\text{H}$  NMR (600 MHz,  $\text{CDCl}_3$ )  $\delta$  13.01 (1H, s, chelated-OH), 8.08–8.03 (1H, m, naphthalene-H), 7.97–7.92 (1H, m, naphthalene-H), 7.68 (1H, d,  $J = 7.9$  Hz, 2'-H), 7.67–7.61 (2H, m, naphthalene-H), 7.40 (1H, d,  $J = 7.9$  Hz, 3'-H), 6.80 (1H, s, 3-H), 2.68 (2H, d,  $J = 7.1$  Hz), 2.48 (2H, q,  $J = 7.4$  Hz), 2.43–2.32 (1H, m), 2.24–2.13 (2H, m), 1.94–1.84 (2H, m), 1.15 (6H, d,  $J = 6.6$  Hz), 1.06 (3H, t,  $J = 7.4$  Hz), 0.72 (6H, t,  $J = 7.4$  Hz). HRMS  $m/z$  489.2289 [ $\text{M}+\text{H}$ ] $^+$  (calcd for  $\text{C}_{30}\text{H}_{32}\text{O}_6$ , 489.2272).



**4.1.2.4. 4'-Butyryloxynaphthalen-1'-yl-TEDB (9):**  $^1\text{H}$  NMR (300 MHz,  $\text{CDCl}_3$ )  $\delta$  13.01 (s, 1H, chelated-OH), 8.08–8.02 (1H, m, naphthalene-H), 7.98–7.92 (1H, m, naphthalene-H), 7.69 (1H, d,  $J = 8.0$  Hz, 2'-H), 7.68–7.61 (2H, m, naphthalene-H), 7.40 (1H, d,  $J = 8.0$  Hz, 3'-H), 6.80 (1H, s, 3-H), 2.78 (2H, t,  $J = 7.3$  Hz), 2.49 (2H, q,  $J = 7.4$  Hz), 2.24–2.13 (2H, m), 1.99–1.84 (4H, m), 1.14 (3H, t,  $J = 7.3$  Hz), 1.06 (3H, t,  $J = 7.4$  Hz), 0.72 (6H, t,  $J = 7.4$  Hz). HRMS  $m/z$  475.2121  $[\text{M}+\text{H}]^+$  (calcd for  $\text{C}_{29}\text{H}_{30}\text{O}_6$ ).

**4.1.2.5. 4'-Benzyloxynaphthalen-1'-yl-TEDB (10):**  $^1\text{H}$  NMR (300 MHz,  $\text{CDCl}_3$ )  $\delta$  13.00 (1H, s, chelated-OH), 7.91 (1H, d,  $J = 8.4$  Hz, Ph-H), 7.76 (1H, d,  $J = 8.4$  Hz, Ph-H), 7.66 (1H, d,  $J = 7.8$  Hz, 2'-H), 7.60 (1H, dd,  $J = 7.8$  and 7.0 Hz, Ar-H), 7.54 (1H, d,  $J = 7.8$  Hz, 3'-H), 7.52–7.48 (2H, m, naphthalene-H), 7.44 (2H, dd,  $J = 7.8$  and 7.0 Hz, Ar-H), 7.42–7.35 (2H, m, Ar-H), 6.78 (1H, s, 3-H), 4.07 (2H, s,  $-\text{CH}_2\text{Ph}$ ), 2.48 (2H, q,  $J = 7.4$  Hz), 2.24–2.12 (2H, m), 1.94–1.82 (2H, m), 1.06 (3H, t,  $J = 7.4$  Hz), 0.71 (6H, t,  $J = 7.4$  Hz). HRFABMS  $m/z$  523.2128  $[\text{M}+\text{H}]^+$  (calcd for  $\text{C}_{33}\text{H}_{30}\text{O}_6$ , 523.2121).

**4.1.2.6. 4'-Phenylpropanoyloxynaphthalen-1'-yl-TEDB (11):**  $^1\text{H}$  NMR (300 MHz,  $\text{CDCl}_3$ )  $\delta$  13.00 (1H, s, chelated-OH), 7.91 (1H, d,  $J = 8.2$  Hz, Ar-H), 7.70 (1H, d,  $J = 8.4$  Hz, Ar-H), 7.65 (1H, d,  $J = 7.8$  Hz, Ar-H), 7.61 (1H, dd,  $J = 8.4$  and 7.0 Hz, Ar-H), 7.54 (1H, dd,  $J = 8.2$  and 7.0 Hz, Ar-H), 7.41–7.25 (6H, m, Ar-H), 6.79 (1H, s, 3-H), 3.24–3.09 (4H, m), 2.48 (2H, q,  $J = 7.3$  Hz), 2.24–2.11 (2H, m), 1.94–1.82 (2H, m), 1.06 (3H, t,  $J = 7.3$  Hz), 0.72 (6H, t,  $J = 7.3$  Hz). HRMS  $m/z$  537.2295  $[\text{M}+\text{H}]^+$  (calcd for  $\text{C}_{34}\text{H}_{32}\text{O}_6$ , 537.2272).

**4.1.2.7. 4'-Benzoyloxynaphthalen-1'-yl-TEDB (12):**  $^1\text{H}$  NMR (400 MHz,  $\text{CDCl}_3$ )  $\delta$  13.02 (1H, s, chelated-OH), 8.35 (2H, d,  $J = 7.2$  Hz, Ph-H), 8.15–8.09 (2H, m, Ph-H), 8.01–7.92 (1H, m, naphthalene-H), 7.75 (1H, d,  $J = 7.9$  Hz, 2'-H), 7.68–7.58 (2H, m, naphthalene-H), 7.53 (1H, d,  $J = 7.9$  Hz, 3'-H), 7.48 (2H, t,  $J = 7.9$  Hz, naphthalene-H), 6.85 (1H, s, 3-H), 2.49 (2H, q,  $J = 7.4$  Hz), 2.26–2.15 (2H, m), 1.98–1.86 (2H, m), 1.07 (3H, t,  $J = 7.4$  Hz), 0.74 (6H, t,  $J = 7.4$  Hz). HRMS  $m/z$  509.1969  $[\text{M}+\text{H}]^+$  (calcd for  $\text{C}_{32}\text{H}_{28}\text{O}_6$ , 509.1959).

**4.1.2.8. 4'-Cinnamoyloxynaphthalen-1'-yl-TEDB (13):**  $^1\text{H}$  NMR (400 MHz,  $\text{CDCl}_3$ )  $\delta$  13.02 (1H, s, chelated-OH), 8.15–8.10 (1H, m, naphthalene-H), 8.04 (1H, d,  $J = 16.0$  Hz), 8.00–7.94 (1H, m, naphthalene-H), 7.3 (1H, d,  $J = 8.0$  Hz, 2'-H), 7.70–7.63 (4H, m, Ph-H), 7.52–7.46 (4H, m, Ph-H), 6.84 (1H, d,  $J = 16.0$  Hz), 6.83 (1H, s, 3-H), 2.49 (2H, q,  $J = 7.4$  Hz), 2.26–2.14 (2H, m), 1.97–1.86 (2H, m), 1.07 (3H, t,  $J = 7.4$  Hz), 0.74 (6H, t,  $J = 7.4$  Hz). HRMS  $m/z$  535.2118  $[\text{M}+\text{H}]^+$  (calcd for  $\text{C}_{34}\text{H}_{30}\text{O}_6$ , 535.2115).

**4.1.2.9. 4'-Dimethylacryloxynaphthalen-1'-yl-TEDB (14):**  $^1\text{H}$  NMR (400 MHz,  $\text{CDCl}_3$ )  $\delta$  13.04 (1H, s, chelated-OH), 8.11–8.05 (1H, m, naphthalene-H), 7.98–7.91 (1H, m, naphthalene-H), 7.69 (1H, d,  $J = 7.8$  Hz, 2'-H), 7.66–7.60 (2H, m, naphthalene-H), 7.41 (1H, d,  $J = 7.8$  Hz, 3'-H), 6.81 (1H, s, 3-H), 6.18–6.15 (1H, m), 2.48 (2H, q,  $J = 7.4$  Hz), 2.29 (3H, d,  $J = 1.2$  Hz), 2.24–2.14 (2H, m), 2.09 (3H, d,  $J = 1.2$  Hz), 1.95–1.84 (2H, m), 1.06 (3H, t,  $J = 7.4$  Hz), 0.72 (6H, t,  $J = 7.3$  Hz). HRMS  $m/z$   $[\text{M}+\text{H}]^+$  487.2121 (calcd for  $\text{C}_{30}\text{H}_{30}\text{O}_6$ , 487.2115).

**4.1.2.10. 2'-Acetoxynaphthalen-1'-yl-TEDB (15):**  $^1\text{H}$  NMR (400 MHz,  $\text{CDCl}_3$ )  $\delta$  12.93 (1H, s, chelated-OH), 8.08 (1H, d,  $J = 9.1$  Hz, naphthalene-H), 7.99–7.94 (1H, m, naphthalene-H), 7.61–4.56 (3H, m, naphthalene-H), 7.35 (1H, d,  $J = 9.1$  Hz, naphthalene-H), 6.68 (1H, s, 3-H), 2.48 (2H, q,  $J = 7.4$  Hz), 2.26 (3H, s), 2.18–2.07 (2H, m), 1.88–1.76 (2H, m), 1.06 (3H, t,  $J = 7.4$  Hz), 0.70 (6H, t,  $J = 7.3$  Hz). HRMS  $m/z$  447.1795  $[\text{M}+\text{H}]^+$  (calcd for  $\text{C}_{27}\text{H}_{26}\text{O}_6$ , 447.1802).

**4.1.2.11. 2'-Propionyloxynaphthalen-1'-yl-TEDB (16):**  $^1\text{H}$  NMR (300 MHz,  $\text{CDCl}_3$ )  $\delta$  12.93 (1H, s, chelated-OH), 8.08 (1H, d,  $J = 9.0$  Hz, naphthalene-H), 7.99–7.94 (1H, m, naphthalene-H), 7.61–4.56 (3H, m, naphthalene-H), 7.34 (1H, d,  $J = 9.0$  Hz, naphthalene-H), 6.66 (1H, s, 3-H), 2.54 (2H, q,  $J = 7.6$  Hz), 2.48 (2H, q,  $J = 7.4$  Hz), 2.18–2.06 (2H, m), 1.87–1.76 (2H, m), 1.20 (3H, t,  $J = 7.6$  Hz<sub>3</sub>), 1.06 (3H, t,  $J = 7.4$  Hz), 0.70 (6H, t,  $J = 7.4$  Hz). HRMS  $m/z$  461.1952  $[\text{M}+\text{H}]^+$  (calcd for  $\text{C}_{28}\text{H}_{28}\text{O}_6$ , 461.1959).

**4.1.2.12. 2'-Benzoyloxynaphthalen-1'-yl-TEDB (17):**  $^1\text{H}$  NMR (400 MHz,  $\text{CDCl}_3$ )  $\delta$  12.86 (1H, s, chelated-OH), 8.16–8.01 (3H, m, Ar-H), 8.02–7.95 (1H, m, Ar-H), 7.69–7.42 (7H, m, Ar-H), 6.72 (1H, s, 3-H), 2.42 (2H, q,  $J = 7.3$  Hz), 2.12–2.00 (2H, m), 1.84–1.72 (2H, m), 1.01 (t, 3H,  $J = 7.3$  Hz), 0.51 (6H, t,  $J = 7.3$  Hz). HRMS  $m/z$  509.1976  $[\text{M}+\text{H}]^+$  (calcd for  $\text{C}_{32}\text{H}_{28}\text{O}_6$ , 509.1959).

**4.1.2.13. 2'-Cinnamoyloxynaphthalen-1'-yl-TEDB (18):**  $^1\text{H}$  NMR (400 MHz,  $\text{CDCl}_3$ )  $\delta$  12.92 (1H, s, chelated-OH), 8.11 (1H, d,  $J = 9.1$  Hz, naphthalene-H), 8.00–7.94 (1H, m, naphthalene-H), 7.83 (1H, d,  $J = 16.0$  Hz), 7.63–7.36 (9H, m, Ar-H), 6.55 (1H, d,  $J = 16.0$  Hz), 6.82 (1H, s, 3-H), 2.44 (2H, q,  $J = 7.4$  Hz), 2.16–2.04 (2H, m), 1.89–1.79 (2H, m), 1.03 (3H, t,  $J = 7.4$  Hz), 0.66 (6H, t,  $J = 7.4$  Hz). HRMS  $m/z$  535.2138  $[\text{M}+\text{H}]^+$  (calcd for  $\text{C}_{34}\text{H}_{30}\text{O}_6$ , 535.2115).

**4.1.2.14. 6'-Acetoxynaphthalen-2'-yl-TEDB (19):**  $^1\text{H}$  NMR (400 MHz,  $\text{CDCl}_3$ )  $\delta$  13.05 (1H, s, chelated-OH), 8.31 (1H, br s, naphthalene-H), 8.01 (1H, d,  $J = 8.8$  Hz, naphthalene-H), 7.97 (1H, d,  $J = 8.8$  Hz, naphthalene-H), 7.81 (1H, dd,  $J = 8.8$  and 1.8 Hz, naphthalene-H), 7.67 (1H, d,  $J = 2.2$  Hz, naphthalene-H), 7.38 (1H, dd,  $J = 8.8$  and 2.2 Hz, naphthalene-H), 7.02 (1H, s, 3-H), 2.47 (2H, q,  $J = 7.4$  Hz), 2.39 (3H, s), 2.37–2.25 (2H, m), 2.11–2.01 (2H, m), 1.06 (3H, t,  $J = 7.4$  Hz), 0.71 (6H, t,  $J = 7.4$  Hz). HRMS  $m/z$  447.1798  $[\text{M}+\text{H}]^+$  (calcd for  $\text{C}_{27}\text{H}_{26}\text{O}_6$ , 447.1802).

**4.1.2.15. 6'-Propionyloxynaphthalen-2'-yl-TEDB (20):**  $^1\text{H}$  NMR (300 MHz,  $\text{CDCl}_3$ )  $\delta$  13.06 (1H, s, chelated-OH), 8.31 (1H, br s, naphthalene-H), 8.01 (1H, d,  $J = 8.9$  Hz, naphthalene-H), 7.96 (1H, d,  $J = 8.9$  Hz, naphthalene-H), 7.81 (1H, dd,  $J = 8.9$  and 1.9 Hz, naphthalene-H), 7.67 (1H, d,  $J = 2.3$  Hz, naphthalene-H), 7.38 (1H, dd,  $J = 8.9$  and 2.3 Hz, naphthalene-H), 7.02 (1H, s, 3-H), 2.69 (2H, q,  $J = 7.4$  Hz<sub>3</sub>), 2.48 (2H, q,  $J = 7.4$  Hz<sub>3</sub>), 2.36–2.24 (2H, m), 2.12–2.00 (2H, m), 1.33 (3H, t,  $J = 7.4$  Hz<sub>3</sub>), 1.06 (3H, t,  $J = 7.4$  Hz<sub>3</sub>), 0.71 (6H, t,  $J = 7.4$  Hz). HRMS  $m/z$  461.1952  $[\text{M}+\text{H}]^+$  (calcd for  $\text{C}_{28}\text{H}_{28}\text{O}_6$ , 461.1959).

**4.1.2.16. 6'-Benzoyloxynaphthalen-2'-yl-TEDB (21):**  $^1\text{H}$  NMR (400 MHz,  $\text{CDCl}_3$ )  $\delta$  13.06 (1H, s, chelated-OH), 8.35 (1H, br s, naphthalene-H), 8.26 (2H, d,  $J = 8.8$  Hz, Ar-H), 8.07 (1H, d,  $J = 8.8$  Hz, Ar-H), 8.00 (1H, d,  $J = 8.6$  Hz, Ar-H), 7.86–7.80 (2H, m, Ar-H),

7.74–7.66 (1H, m, Ar-H), 7.60–7.50 (3H, m, Ar-H), 7.04 (1H, s, 3-H), 2.49 (2H, q,  $J = 7.4$  Hz), 2.39–2.26 (2H, m), 2.14–2.02 (2H, m), 1.06 (3H, t,  $J = 7.3$  Hz), 0.72 (6H, t,  $J = 7.3$  Hz). HRMS  $m/z$  509.1963 [M+H]<sup>+</sup> (calcd for C<sub>32</sub>H<sub>28</sub>O<sub>6</sub>, 509.1959).

**4.1.2.17. 6'-Cinnamoyloxynaphthalen-2'-yl-TEDB (22):** <sup>1</sup>H NMR (400 MHz, CDCl<sub>3</sub>)  $\delta$  13.07 (1H, s, chelated-OH), 8.33 (1H, br s, naphthalene-H), 8.04 (2H, d,  $J = 8.8$  Hz, Ar-H), 8.00 (1H, d,  $J = 8.7$  Hz, Ar-H), 7.95 (1H, d,  $J = 16.0$  Hz, -COCH=CH-Ph), 7.82 (1H, dd,  $J = 8.7$  and  $2.0$  Hz, Ar-H), 7.67 (1H, d,  $J = 2.0$  Hz, Ar-H), 7.66–7.60 (2H, m, Ar-H), 7.50–7.44 (3H, m, Ar-H), 7.03 (1H, s, 3-H), 6.90 (1H, d,  $J = 16.0$  Hz), 2.48 (2H, q,  $J = 7.4$  Hz), 2.37–2.26 (2H, m, 8-CH<sub>2</sub>CH<sub>3</sub>), 2.13–2.02 (2H, m), 1.06 (3H, t,  $J = 7.4$  Hz), 0.71 (6H, t,  $J = 7.4$  Hz). HRMS  $m/z$  535.2111 [M+H]<sup>+</sup> (calcd for C<sub>34</sub>H<sub>30</sub>O<sub>6</sub>, 535.2115).

## 4.2. Biology

**4.2.1. Antiproliferative Activity Assay**—Antiproliferative activity of analogues was performed as described before.<sup>7</sup> Briefly, all stock cell lines were grown in T-75 flasks at 37 °C with 5% CO<sub>2</sub> in air. Freshly trypsinized cell suspensions were seeded in 96-well microtiter plates at densities of 7,500–25,000 cells per well with compounds. Compounds were prepared in DMSO and diluted by culture medium. The highest concentration of DMSO in the cultures (0.1% v/v) was without effect on cell growth under the culture conditions used. After 72 h in culture with test compounds, cells were fixed in 10% trichloroacetic acid and then stained with 0.04% sulforhodamine B. The absorbance at 515 nm was measured using a microplate reader (ELx800, BioTek) operated by Gen5 software (BioTek) after solubilizing the bound dye with 10 mM Tris base. The IC<sub>50</sub> was calculated from at least three independent experiments performed with duplication. The following human tumor cell lines were used in the assay: A549 (lung carcinoma), Hep G2 (hepatocellular carcinoma), HCT-8 (colon adenocarcinoma), KB (originally isolated from epidermoid carcinoma of the nasopharynx), and KB-VIN (vincristine-resistant KB subline showing MDR phenotype by overexpressing P-gp), PC-3 (androgen-insensitive prostate cancer), SK-BR-3 (ER-negative, progesterone receptor (PgR)-negative, HER2-overexpressing breast cancer). All cell lines were obtained from the Lineberger Comprehensive Cancer Center (UNC-CH) or from ATCC (Manassas, VA), except KB-VIN, which was a generous gift from Professor Y.-C. Cheng (Yale University). Cells were cultured in RPMI-1640 medium supplemented with 2 mM L-glutamine and 25 mM HEPES (Mediatech), supplemented with 10% heat-inactivated fetal bovine serum (Hyclone), 100  $\mu$ g/mL streptomycin, and 100 IU penicillin. MDR stock cells (KB-VIN) were maintained in the presence of 100 nM vincristine.

**4.2.2. Tubulin assays**—Inhibitory effects of compounds against tubulin polymerization were evaluated as described previously, using purified bovine brain tubulin.<sup>9)</sup> Tubulin assembly was measured by turbidimetry at 350 nm. Assay mixtures contained 1.0 mg/mL (10  $\mu$ M) tubulin and varying compound concentrations and were preincubated 15 min at 30 °C without guanosine 5'-triphosphate (GTP). The samples were placed on ice, and 0.4 mM GTP was added. Reaction mixtures were transferred to 0 °C cuvettes, and turbidity development was followed for 20 min at 30 °C following a rapid temperature jump. Compound concentrations as EC<sub>50</sub> values that inhibited increase in turbidity by 50% relative

to a control sample were determined. Inhibition of the binding of [<sup>3</sup>H]colchicine to purified tubulin was measured as described previously.<sup>10</sup> Tubulin (1.0 μM) was incubated with 5.0 μM [<sup>3</sup>H]colchicine and 5.0 μM test compound at 37 °C for 10 min, when about 40–60% of maximum colchicine binding occurs in control samples.

**4.2.3. Cell Cycle Analysis**—Distribution of cells in the cell cycle was evaluated by measurement of cellular DNA content with propidium iodide (PI) (BD Biosciences) as described previously.<sup>7</sup> Briefly, cells were seeded in a 12-well culture plate 24 h prior to treatment with compounds. Both KB and KB-VIN cells were treated with 1 and 10 μM **3**, **4**, **6**, **7**, **12**, **16**, or **18**, 10 and 40 μM **13**, 0.2 μM CA-4, or vehicle (DMSO) as a control. Stained cells were analyzed by flow cytometry (BD FACSCalibur, BD Biosciences). Experiments were repeated a minimum of three times.

**4.2.4. Immunofluorescence Staining**—Immunostaining of KB-VIN was performed as described previously.<sup>7</sup> Briefly, KB-VIN cells were grown on an 8-well chamber slide (Lab-Tech) for 24 h prior to treatment with reagents. Cells were treated with reagent for 24 h. Concentrations of reagents were determined at their IC<sub>50</sub> and/or effective concentration used for cell cycle analysis as follows: 0.2 μM combretastatin A-4, 10 μM for **3** and **4**, 10 and 40 μM for **16** and **18**, and DMSO as a control. Cells were fixed in 4% paraformaldehyde in PBS, and permeabilized with 0.5% Triton X-100 in PBS. Fixed cells were labeled with mouse monoclonal antibody to α-tubulin (B5-1-2, Sigma) and rabbit IgG to Ser10-phosphorylated histone H3 (p-H3) (#06-570, EMD Millipore), followed by FITC-conjugated antibody to mouse IgG (Sigma) and Alexa Fluor 549-conjugated antibody to rabbit IgG (Life Technologies). Nuclei were labeled with DAPI (Sigma). Fluorescence labeled cells were observed using a confocal microscope (Zeiss, LSM700) controlled by ZEN software (Zeiss). Confocal images were stacked and merged using ZEN (black edition) software. Final images were prepared using Photoshop CS6 (Adobe).

### 4.3. Computer Modeling

Three-dimensional (3D) structures of tubulin-ligand complexes were modeled by GOLD 5.1 software<sup>11</sup> with default settings. The 3D structure of human tubulin (TUBA1A and TUBB2B) used in this study was constructed from the Protein DataBank (PDB) entry (PDB ID: 1SA0).<sup>12</sup> Missing hydrogen atoms in the crystal structure were computationally added by Hermes.<sup>13</sup> The center of the active site was defined as the center of the ligand in 1SA0, and the active site radius was set to 10.0 Å. For the docking calculations, the quantum-chemically optimized structures of ligands were used as initial structures. The structural optimizations of ligands were carried out by B3LYP/6-311+G(df,p) using Gaussian 09, Revision B.01.<sup>14</sup>

## Supplementary Material

Refer to Web version on PubMed Central for supplementary material.

## Acknowledgments

We wish to thank the Microscopy Service Laboratory (UNC-CH) for their expertise in fluorescence and confocal microscopy. In addition, we appreciate critical comments, suggestions, and editing of the manuscript by Dr. Susan L. Morris-Natschke (UNC-CH). This study was supported by Grant-in-Aid from the Ministry of Education, Culture, Sports, Science and Technology (MEXT KAKENHI, Japan), awarded to K.N.G. (Grant Number 25293024 & 25670054) and A.O. (Grant Number 26460034 & 15H01064), as well as by a grant from the Terumo Life Science Foundation awarded to K.N.G. This work was supported in part by NIH grant CA177584 from the National Cancer Institute awarded to K.H.L. This work was also supported by a grant from the University Research Council (UNC), and the IBM Junior Faculty Development Award, as well as the Eshelman Institute for Innovation, Chapel Hill, North Carolina, awarded to M.G. The content of this paper is solely the responsibility of the authors and does not necessarily reflect the official views of the National Institutes of Health.

## References and notes

1. Newman DJ, Cragg GM. *J Nat Prod.* 2016; 79:629. [PubMed: 26852623]
2. Nakagawa-Goto K, Bastow KF, Wu JH, Tokuda H, Lee KH. *Bioorg Med Chem Lett.* 2005; 15:3016. [PubMed: 15913998]
3. Nakagawa-Goto K, Bastow KF, Chen TH, Morris-Natschke SL, Lee KH. *J Med Chem.* 2008; 51:3297. [PubMed: 18473435]
4. Nakagawa-Goto K, Chang PC, Lai CY, Hung HY, Chen TH, Wu PC, Zhu H, Sedykh A, Bastow KF, Lee KH. *J Med Chem.* 2010; 53:6699. [PubMed: 20735140]
5. Kuo TC, Chiang PC, Yu CC, Nakagawa-Goto K, Bastow KF, Lee KH, Guh JH. *Biochem Pharmacol.* 2011; 81:1136. [PubMed: 21371443]
6. Nakagawa-Goto K, Wu PC, Lai CY, Hamel E, Zhu H, Zhang L, Kozaka T, Ohkoshi E, Goto M, Bastow KF, Lee KH. *J Med Chem.* 2011; 54:1244. [PubMed: 21284385]
7. Nakagawa-Goto K, Oda A, Hamel E, Ohkoshi E, Lee KH, Goto M. *J Med Chem.* 2015; 58:2378. [PubMed: 25695315]
8. Kingston, DGI. Taxol and its analogs. In: Cragg, GM.; Kingston, DGI.; Newman, DJ., editors. *Anticancer Agents from Natural Products.* 2. CRC Press; Boca Raton, FL: 2011.
9. Hamel E. *Cell Biochem Biophys.* 2003; 38:1. [PubMed: 12663938]
10. Verdier-Pinard P, Lai JY, Yoo HD, Yu J, Márquez B, Nagle DG, Nambu M, White JD, Falck JR, Gerwick WH, Day BW, Hamel E. *Mol Pharmacol.* 1998; 53:62. [PubMed: 9443933]
11. Jones G, Willett P, Glen RC. *J Mol Biol.* 1995; 245:43. [PubMed: 7823319]
12. Ravelli RB, Gigant B, Curmi PA, Jourdain I, Lachkar S, Sobel A, Knossow M. *Nature.* 2004; 428:198. [PubMed: 15014504]
13. Hermes 5.1. CCDC Software Ltd; Cambridge, UK: 2012.
14. Frisch, MJ.; Trucks, GW.; Schlegel, HB.; Scuseria, GE.; Robb, MA.; Cheeseman, JR.; Scalmani, G.; Barone, V.; Mennucci, B.; Petersson, GA.; Nakatsuji, H.; Caricato, M.; Li, X.; Hratchian, HP.; Izmaylov, AF.; Bloino, J.; Zheng, G.; Sonnenberg, JL.; Hada, M.; Ehara, M.; Toyota, K.; Fukuda, R.; Hasegawa, J.; Ishida, M.; Nakajima, T.; Honda, Y.; Kitao, O.; Nakai, H.; Vreven, T.; Montgomery, JA.; Peralta, JE., Jr; Ogliaro, F.; Bearpark, M.; Heyd, JJ.; Brothers, E.; Kudin, KN.; Staroverov, VN.; Keith, T.; Kobayashi, R.; Normand, J.; Raghavachari, K.; Rendell, A.; Burant, JC.; Iyengar, SS.; Tomasi, J.; Cossi, M.; Rega, N.; Millam, JM.; Klene, M.; Knox, JE.; Cross, JB.; Bakken, V.; Adamo, C.; Jaramillo, J.; Gomperts, R.; Stratmann, RE.; Yazyev, O.; Austin, AJ.; Cammi, R.; Pomelli, C.; Ochterski, JW.; Martin, RL.; Morokuma, K.; Zakrzewski, VG.; Voth, GA.; Salvador, P.; Dannenberg, JJ.; Dapprich, S.; Daniels, AD.; Farkas, O.; Foresman, JB.; Ortiz, JV.; Cioslowski, J.; Fox, DJ. *Gaussian 09 (Revision B.01).* Gaussian, Inc; Wallingford, CT: 2010.

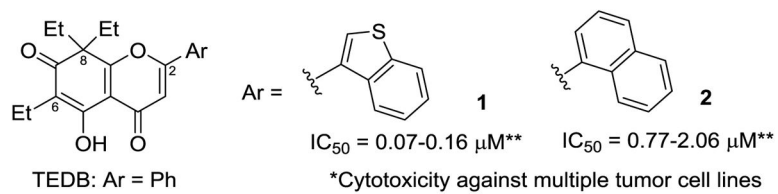


**Figure 1.**  
Structures of TEDB-TB Analogues



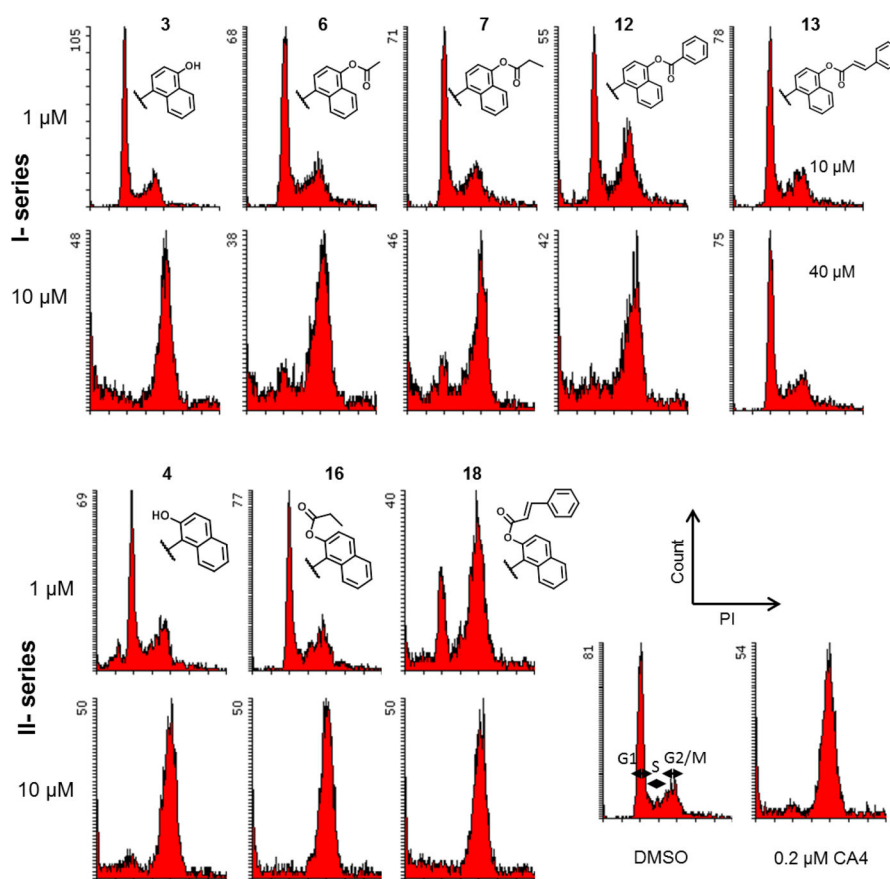


**Figure 2. Induction of cell cycle arrest at G2/M**

KB-VIN cells were treated with the indicated compound for 24 h at the indicated concentrations. Harvested cells were subjected to flow cytometry after staining with propidium iodide (PI). DMSO and 0.2  $\mu\text{M}$  of CA-4 were used as a negative control and an antitubulin agent arresting cells at G2/M, respectively.

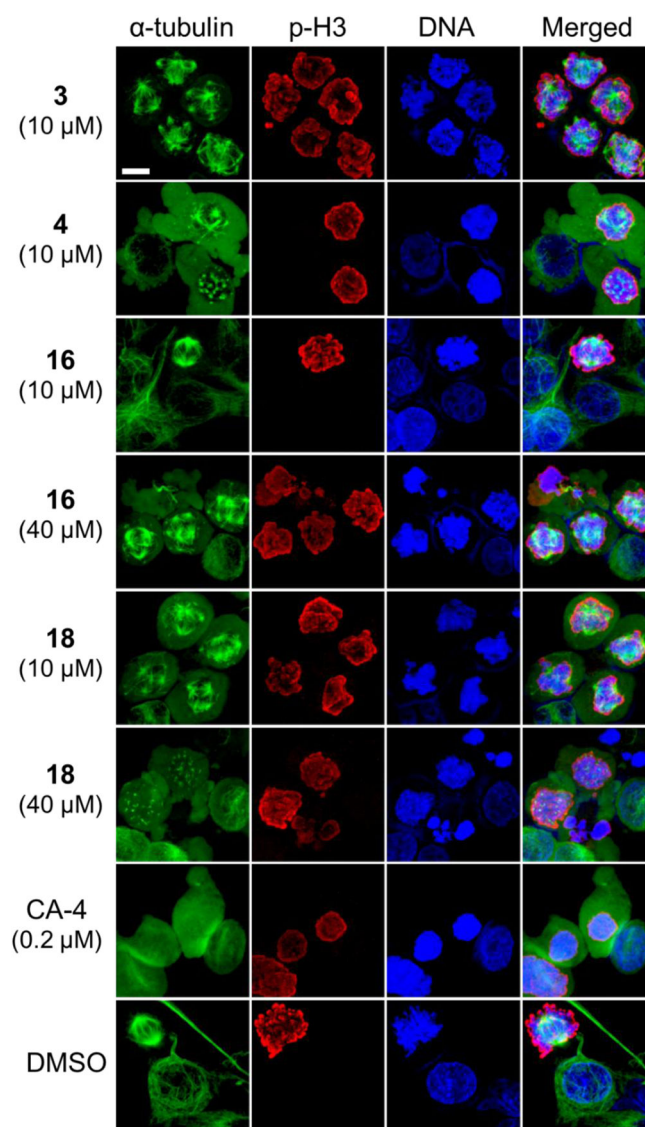


**Figure 3. Effects of compounds on microtubule and spindle formation in KB-VIN cells in a dose dependent manner**

KB-VIN cells were treated for 24 h with compound (**3**, **4**, **16**, or **18**) at the indicated concentrations. CA-4 or DMSO was used as a positive control for a colchicine site antitubulin agent or negative control, respectively. Fixed cells were stained with antibodies to  $\alpha$ -tubulin (green) and serine 10-phosphorylated histone H3 (p-H3, red) as a chromosome condensation marker, DAPI was used for DNA (blue). Stacked and merged confocal images are presented. Bar, 10  $\mu$ m.

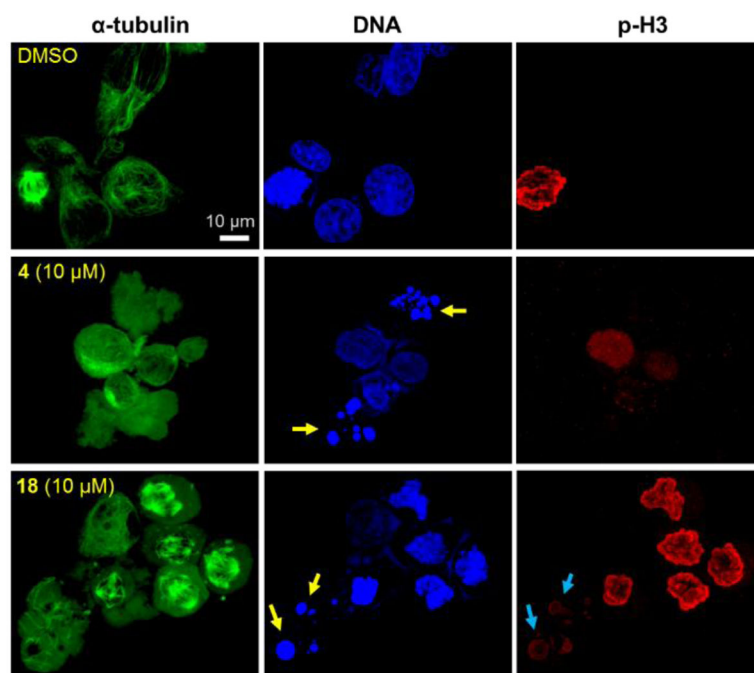


**Figure 4. Induction of nuclear fragmentation by 4 and 18**  
KB-VIN cells were treated for 24 h with **4** or **18** at 10  $\mu$ M followed by fixing by PFA, staining with antibodies to  $\alpha$ -tubulin (green) and chromosome condensation marker p-H3 (red), and DAPI (blue) was used for DNA. Bar, 10  $\mu$ m.

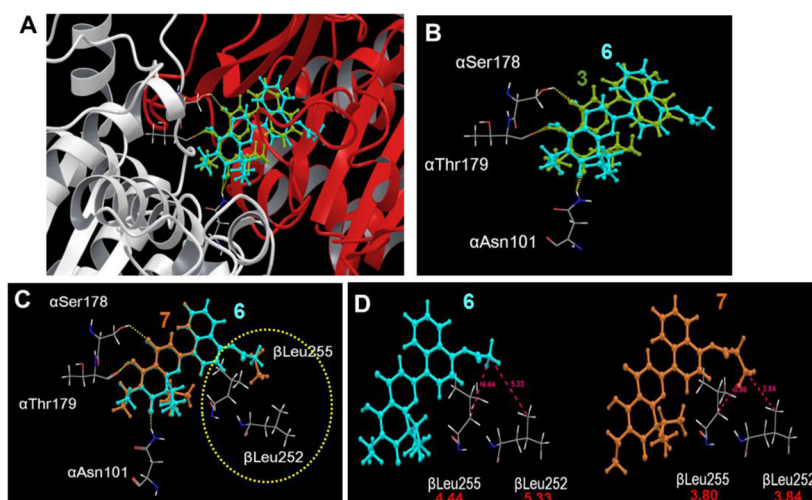


**Figure 5. Docking model of 4'-analogues in the colchicine site**

(A) Docking model of **3** (green) and **6** (blue) in the colchicine site (CS) of the  $\alpha$ -tubulin (white ribbon)/ $\beta$ -tubulin (red ribbon) crystal structure (PDB ID: 1SA0). (B) Superimposition of docked compounds **3** (green) and **6** (blue). (C) Superimposition of docked compounds **6** (blue) and **7** (orange). (D) The distances (red dotted lines) between compounds and amino acid residues in  $\beta$ -tubulin.

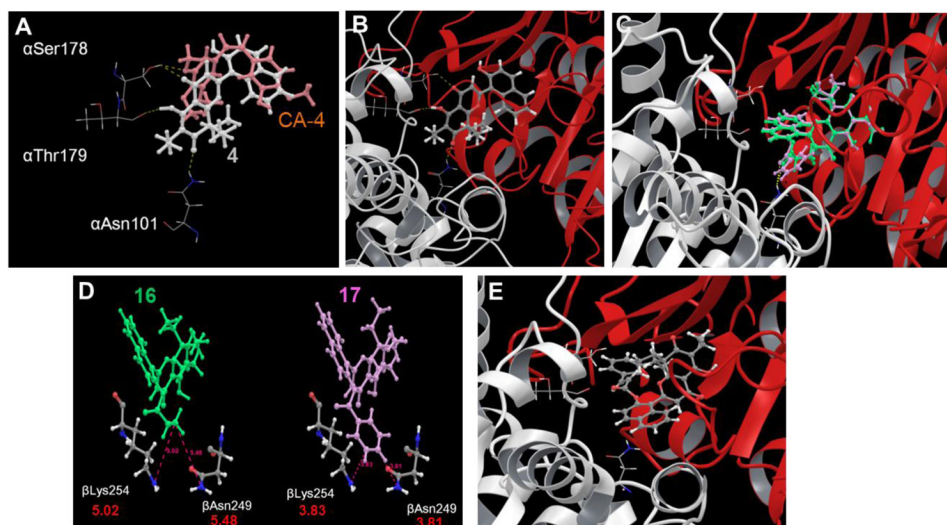


**Figure 6. Docking model of 2'-analogues in the colchicine site**  
(A) Comparison of the docking mode of **4** (white) and CA-4 (orange) in the CS. (B & C) Superimposition of docked compounds **4** (gray skeleton with oxygen in red, hydrogen in white) (B), **16** (green), and **17** (pink) (C) in the CS of  $\alpha$ - (gray ribbon) and  $\beta$ -tubulin (red ribbon) dimer. (D) The distances (red dotted lines) between compounds and amino acid residues in  $\beta$ -tubulin. (E) Superimposition of docked **18** (gray skeleton with oxygen in red, hydrogen in white) in the CS.

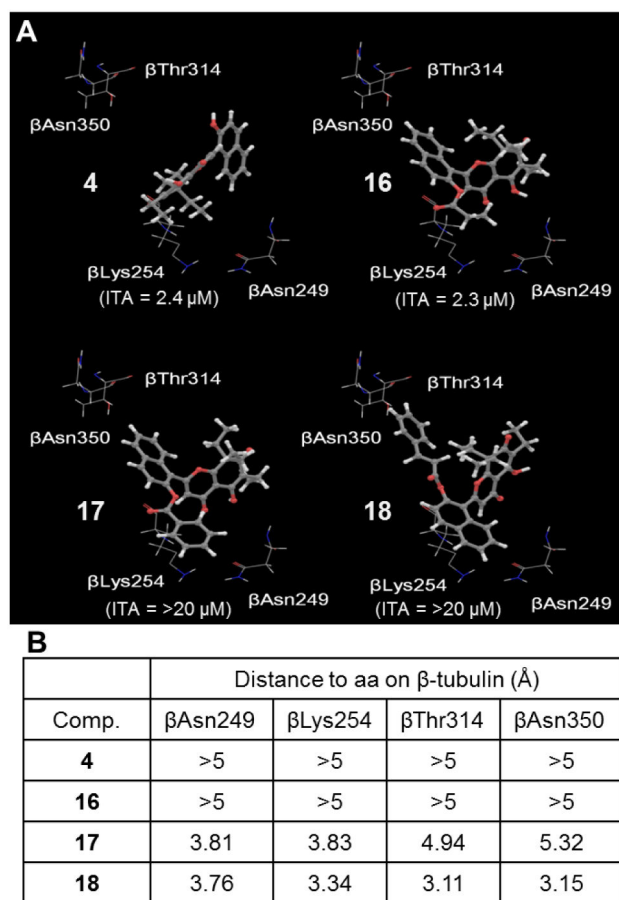
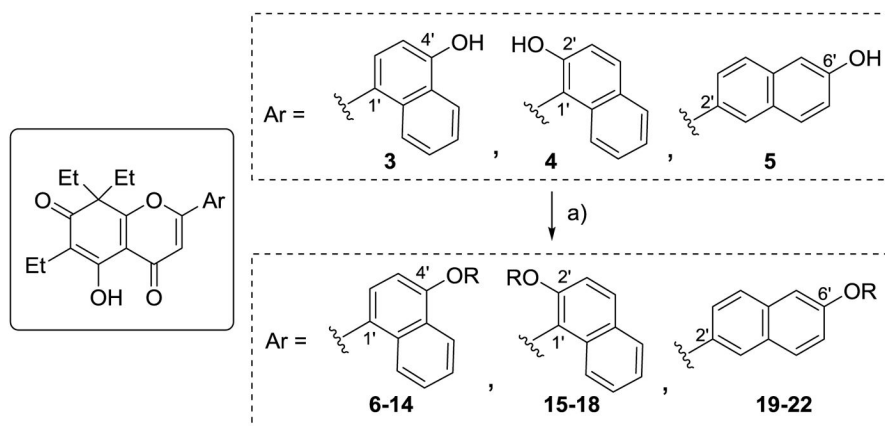


**Figure 7.** Role of steric hindrance for docking to the colchicine site. (A) Possible steric hindrance between compounds **4**, **16**, **17**, or **18** (gray skeleton with oxygen in red, hydrogen in white) and the CS. (B) The calculated distances between each compound (Comp.) and amino acid (aa) are denoted in  $\text{\AA}$ .





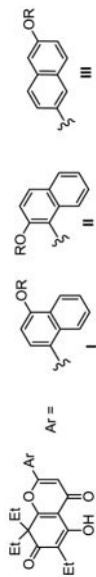
**Scheme 1. Syntheses of New Analogues 6-22.**

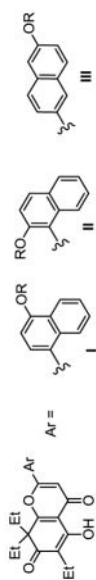
Reagents and conditions: a)  $\text{Et}_3\text{N}$ ,  $\text{RCl}$  [various acyl chlorides, such as acetyl chloride ( $\text{R} = \text{CH}_3\text{CO}$ ), propionyl chloride ( $\text{R} = \text{CH}_3\text{CH}_2\text{CO}$ ), butyryl chloride ( $\text{R} = \text{CH}_3\text{CH}_2\text{CH}_2\text{CO}$ ), benzoyl chloride ( $\text{R} = \text{PhCO}$ ), cinnamoyl chloride ( $\text{R} = \text{PhCH}=\text{CHCO}$ )]

Table 1

Cytotoxicity and Anti-tubulin Activity of Synthesized Naphthalene Analogues

cell line <sup>a</sup>		A549	HCT-8	Hep G2	PC-3	DU	SK-BR-3	KB	KB-VIN	ITA <sup>b</sup>	ICB <sup>c</sup>
R											
I	3	H	0.9	1.0	0.4	1.1	-	0.7	0.5	3.4	54%
	6	C(O)CH <sub>3</sub>	0.2	0.5	0.3	0.2	5.7	0.2	0.4	2.4	49%
	7	C(O)CH <sub>2</sub> CH <sub>3</sub>	0.9	1.8	0.6	1.1	5.0	0.7	0.6	NA <sup>d</sup>	-e
	8	C(O)CH <sub>2</sub> CH(CH <sub>3</sub> ) <sub>2</sub>	19.5	NA	16.3	NA	15.1	14.6	12.2	-	-
	9	C(O)CH <sub>2</sub> CH <sub>2</sub> CH <sub>3</sub>	1.4	1.4	1.4	2.5	0.9	0.8	0.9	-	-
	10	C(O)CH <sub>2</sub> Ph	1.3	1.1	1.3	2.0	0.7	0.7	0.8	0.7	-
	11	C(O)CH <sub>2</sub> CH <sub>2</sub> Ph	1.3	1.1	1.5	1.9	0.7	0.3	0.8	0.8	-
	12	C(O)Ph	0.2	0.6	0.5	0.2	5.1	4.9	0.1	0.8	NA
	13	C(O)CH=CHPh	1.9	2.4	1.4	1.1	5.4	5.0	1.2	0.2	-
	14	C(O)CH=C(CH <sub>3</sub> ) <sub>2</sub>	0.8	1.7	1.4	1.0	5.3	5.3	1.0	0.8	-
II	4	H	1.2	1.3	1.6	3.0	0.8	0.9	1.0	2.4	55%
	15	C(O)CH <sub>3</sub>	0.6	4.7	5.7	5.2	0.5	0.8	0.5	0.7	-
	16	C(O)CH <sub>2</sub> CH <sub>3</sub>	1.3	4.7	3.5	15.2	0.9	1.1	0.7	2.3	39%
	17	C(O)Ph	1.0	1.1	1.6	3.8	1.1	0.8	0.7	0.9	NA
	18	C(O)CH=CHPh	1.3	4.3	4.9	22.1	0.9	0.9	0.9	0.8	NA
III	5	H	15.0	14.1	13.4	13.0	12.2	14.3	19.9	13.7	-
	19	C(O)CH <sub>3</sub>	12.0	15.4	17.4	15.7	12.7	10.7	12.2	11.0	-
	20	C(O)CH <sub>2</sub> CH <sub>3</sub>	9.0	11.1	13.5	14.8	11.3	9.5	11.9	10.3	-
	21	C(O)Ph	9.5	10.8	NA	16.6	11.0	7.4	11.3	9.9	-
	22	C(O)CH=CHPh	NA	NA	NA	NA	NA	NA	NA	NA	-
		parent compound 2 <sup>7)</sup>	1.6	1.0	2.1	1.0	NT	NT	1.6	0.8	-





cell line <sup>a</sup>	A549	HCT-8	Hep G2	PC-3	DU	SK-BR-3	KB	KB-VIN	ITA <sup>b</sup>	ICB <sup>c</sup>
<b>R</b>										
PXL (nM)	0.7	8.7	10.0	14.5	17.2	12.7	3.8	1720.0	-	-

<sup>a</sup> Antiproliferative activity as IC<sub>50</sub> values (μM) for each cell line, the concentration of compound that caused 50% reduction relative to untreated cells using the sulforhodamine B assay. Human ileocecal colorectal adenocarcinoma (HCT-8), prostate cancer (PC-3, DU 145), lung carcinoma (A549), breast cancer (SK-BR-3), hepatocellular carcinoma (Hep G2), epidermoid carcinoma of the nasopharynx (KB), and its MDR line (KB-VIN).

<sup>b</sup> Inhibition of assembly of purified tubulin, EC<sub>50</sub> (μM) values of 50% inhibition.<sup>9</sup>

<sup>c</sup> Inhibition of colchicine binding, tubulin: 1 μM, [<sup>3</sup>H]colchicine: 5 μM, inhibitor: 5 μM.

<sup>d</sup> NA, not active. Test compound (20μM) did not reach 50% inhibition.

<sup>e</sup> -, not tested.

Results are presented as mean (n = 3), and standard deviations were within 10% for all results.